# Visible Light Active Platinum-Ion-Doped $TiO_2$ Photocatalyst

**Soonhyun Kim,[†,‡] Seong-Ju Hwang,[§] and Wonyong Choi*[,†]**

*School of Environmental Science and Engineering, Pohang University of Science and Technology, Pohang 790-784, South Korea, Daegu Gyeongbuk Institute of Science and Technology, Ducksan-dong, Jung-gu, Daegu 700-742, South Korea, and Division of Nano Sciences and Department of Chemistry, Ewha Womans University, Seoul 120-750, South Korea*

*Received: September 17, 2005; In Final Form: October 24, 2005*

Platinum-ion-doped $TiO_2$ ($Pt_{ion}-TiO_2$) was synthesized by a sol−gel method, and its visible light photocatalytic activities were successfully demonstrated for the oxidative and reductive degradation of chlorinated organic compounds. $Pt_{ion}-TiO_2$ exhibited a yellow-brown color, and its band gap was lower than that of undoped $TiO_2$ by about 0.2 eV. The flat band potential of $Pt_{ion}-TiO_2$ was positively shifted by 50 mV compared with that of undoped $TiO_2$. X-ray absorption spectroscopy and X-ray photoelectron spectroscopy analyses showed that the Pt ions substituted in the $TiO_2$ lattice were present mainly in the Pt(IV) state with some Pt(II) on the sample surface. $Pt_{ion}-TiO_2$ exhibited higher photocatalytic activities than undoped $TiO_2$ under UV irradiation as well. The visible light activity of $Pt_{ion}-TiO_2$ was strongly affected by the calcination temperature and the concentration of Pt ion dopant, which were optimal at 673 K and 0.5 atom %, respectively. Under visible irradiation, $Pt_{ion}-TiO_2$ degraded dichloroacetate and 4-chlorophenol through an oxidative path and trichloroacetate via a reductive path. The activity of $Pt_{ion}-TiO_2$ was not reduced when used repeatedly under visible light. However, visible-light-illuminated $Pt_{ion}-TiO_2$ could not degrade substrates such as tetramethylammonium and trichloroethylene, which are degraded with UV-illuminated $TiO_2$. The characteristics and reactivities of $Pt_{ion}-TiO_2$ as a new visible light photocatalyst were investigated in various ways and discussed in detail.

## Introduction

$TiO_2$ has been extensively investigated as a photocatalyst for the environmental purification of contaminated water and air.[1,2] But it is active only under UV irradiation ($\lambda < 388$ nm), which accounts for less than 5% of solar light energy. There have been various attempts to utilize visible light in $TiO_2$ photocatalysis, which include dye sensitization,[3,4] semiconductor coupling,[5−7] and impurity doping.[8−20]

Doping $TiO_2$ with transition metal ions has been frequently attempted not only to retard the fast charge pair recombination[9−13] but also to enable visible light absorption by providing defect states in the band gap.[8,14−19] In the former case, the UV-excited electrons in the conduction band (CB) or holes in the valence band (VB) are trapped in the defect sites by retarding the recombination and subsequently enhancing the interfacial charge transfers. On the contrary, the intraband states may also serve as recombination centers to decrease the overall photocatalytic activity.[10,11,13,20] In the latter case, the electronic transitions from VB to defect states or from defect states to CB can be allowed under sub-band-gap illumination to show visible activity. However, doping $TiO_2$ with nonmetallic elements is also under active investigation. Recently, Asahi et al.[21] reported that $TiO_2$ doped with nitrogen exhibits visible light reactivity for the degradation of organic compounds. Since this report, carbon,[22] sulfur,[23] nitrogen,[24−26] and boron[27] doping in $TiO_2$ have been successively investigated for their visible light photocatalysis.

Noble metal ions as a dopant have been much less investigated compared with other metal dopants. Noble metals such as Pt, Au, and Ag are usually deposited on the $TiO_2$ surface as a metallic nanoparticle (not as an ionic dopant) to serve as both a CB electron trap and a cocatalyst.[2,28−30] There are only a few reports that studied noble metal ion dopants in the $TiO_2$ lattice. For example, $Au^{3+}$-doped $TiO_2$ exhibited visible light reactivity for methylene blue degradation.[17] Lettmann et al.[31] reported that $TiO_2$ doped with metal ions, such as $Ru^{3+}$, $Rh^{3+}$, $Pt^{4+}$, and $Ir^{3+}$, exhibited visible light activity for the degradation of 4-chlorophenol. Kisch and co-workers also investigated the photocatalytic degradation of 4-chlorophenol under visible irradiation on $TiO_2$ modified with chloride complexes of Pt, Ir, Rh, Au, Pd, Co, and Ni,[32] which is quite different from the typical metal ion-doped titania system. The Pt-chloride-modified titania showed the highest visible activity. They proposed that the surface complexes of metal chlorides serve as visible light absorbing sensitizers and centers of charge separation and that the titania matrix functions as a charge trap.

In this study, we synthesized Pt-ion-doped $TiO_2$ ($Pt_{ion}-TiO_2$) by the sol−gel method and investigated its properties and visible light reactivities for the degradation of several organic compounds. $Pt_{ion}-TiO_2$ exhibited unique characteristics as a new visible light photocatalyst and was clearly different from Pt-metal-deposited $TiO_2$ and Pt-chloride-sensitized $TiO_2$ that have been previously studied.

## Experimental Section

**Chemicals and Materials.** Chemicals used in this study include: 4-chlorophenol (4-CP, Sigma), dichloroacetate (DCA, $CHCl_2CO_2Na$, Aldrich), trichloroacetate (TCA, $CCl_3CO_2Na$, Aldrich), tetramethylammonium (TMA, $N(CH_3)_4Cl$, Acros), trichloroethylene (TCE, Junsei), titanium tetraisopropoxide

* Author to whom correspondence should be addressed. Fax: +82-54-279-8299. E-mail: wchoi@postech.ac.kr.
[†] Pohang University of Science and Technology.
[‡] Daegu Gyeongbuk Institute of Science and Technology.
[§] Ewha Womans University.

10.1021/jp055278y CCC: $30.25 
Published on Web 12/02/2005

(TTIP, $Ti(OCH(CH_3)_2)_4$, Aldrich), ethanol (Aldrich), chloroplatinic acid ($H_2PtCl_6$, Aldrich), nitric acid ($HNO_3$, Shinyo), methyl viologen ($MV^{2+}$, Aldrich), and *tert*-butyl alcohol (TBA, Shinyo). All reagents were used as received.

$Pt_{ion}-TiO_2$ was prepared by a sol−gel method. Approximately 1.25 mL of TTIP dissolved in 25 mL of absolute ethanol was added dropwise to 250 mL of chloroplatinic acid solution (typically 0.08 mM for 0.5 atom % Pt doping) whose pH was adjusted to 1.5 with nitric acid. The resulting colloidal suspension was stirred overnight and then evaporated at 50 °C using a rotavapor. The obtained powder was calcined at various temperatures from 373 to 873 K under air. Undoped $TiO_2$ powder was prepared according to the above procedure in the absence of chloroplatinic acid. Calcined $TiO_2$ powder was washed to remove impurities such as chlorides and nitrates and then dried. Pt-metal-deposited $TiO_2$ ($Pt^0/TiO_2$) was also prepared and compared with $Pt_{ion}-TiO_2$. A photodeposition method was used in obtaining $Pt^0/TiO_2$: A suspension of undoped $TiO_2$ powder (0.5 g/L, as prepared in the above) with 1 M methanol (electron donor) and 30 $\mu$M chloroplatinic acid ($H_2PtCl_6$) was irradiated with a 200-W mercury lamp for 30 min. After irradiation, Pt-deposited $TiO_2$ powder was filtered, washed, and then dried under air. Pt-chloride-sensitized $TiO_2$ ($PtCl_x/TiO_2$) was prepared by adding $H_2PtCl_6$ (30 $\mu$M) to the undoped $TiO_2$ suspension (0.5 g/L, as prepared in the above), then evaporating water and drying under air. $Pt_{ion}-TiO_2$, $Pt^0/TiO_2$, and $PtCl_x/TiO_2$ that are synthesized and compared in this study have mostly anatase matrix in common. Degussa P25, which is a mixture of anatase and rutile (8:2), was also used as a reference photocatalyst.

**Characterization of Catalysts.** X-ray diffraction (XRD, Rigaku model D/Max III) analysis using Cu $K\alpha_1$ radiation was performed to assess the crystallinity of synthesized catalysts. The crystalline region of $TiO_2$ matrix was investigated with high-resolution transmission electron microscopy (HRTEM) and energy-dispersive X-ray (EDX) analysis. The Brunauer−Emmett−Teller (BET) surface area measurements of powder samples were carried out by using $N_2$ as the adsorptive gas. The atomic compositions of $Pt_{ion}-TiO_2$ powders were determined by X-ray photoelectron spectroscopy (XPS) (Kratos XSAM 800pci) using the Mg K$\alpha$ line (1253.6 eV) as the excitation source. The binding energies of all peaks were referenced to the Ti 2p line (458.8 eV) in $TiO_2$ and checked against the C 1s line (284.6 eV) originating from surface impurity carbons. The difference in the binding energies based on the two references was <0.2 eV. X-ray absorption spectroscopy (XAS) experiments were carried out at Pt $L_{III}$ edges by using the extended X-ray absorption fine structure (EXAFS) facility at the Pohang Light Source (PLS) in South Korea, operated at 2.5 GeV and 180 mA. XAS data were collected at room temperature in a transmission mode using gas-ionization detectors. All of the present spectra were calibrated carefully by measuring the reference spectra of Pt metal simultaneously. Data analysis for the spectra was performed by following the standard procedure.[33] Diffuse reflectance UV−vis absorption spectra of the powder samples were obtained using a spectrophotometer (Shimadzu UV-2401PC) equipped with a diffuse reflectance accessory.

For the determination of the flat band potential of $Pt_{ion}-TiO_2$, the photovoltage of suspended $TiO_2$ particles was measured in the presence of methyl viologen.[34,35] A Pt electrode, a saturated calomel electrode (SCE), and a graphite rod were immersed in a reactor as a working, reference, and counter electrode, respectively. Approximately 0.1 g of $TiO_2$ was suspended in 100 mL of distilled water containing 0.1 M $KNO_3$, 1 M sodium acetate, and 1 mM methyl viologen. The suspension pH was adjusted by 1 N NaOH or 1 N $HClO_4$. The suspension was purged with $N_2$ for 30 min and irradiated by UV light. The photovoltage was measured as a function of the suspension pH using a potentiostat (EG&G 263).

**Activity Measurements.** The photocatalytic activities of the synthesized $TiO_2$ powders were evaluated for the photocatalytic degradation (PCD) of DCA, 4-CP, and TCA. $TiO_2$ was dispersed in distilled water (0.5 g/L) by simultaneous sonication and shaking for 30 s in an ultrasonic cleaning bath. An aliquot of the substrate stock solution (1 mM) was subsequently added to the suspension to give a desired substrate concentration, and then the pH of the suspension was adjusted to pH 3 with $HClO_4$ standard solution. When the absence of dissolved oxygen was needed, the reactor was purged with nitrogen gas for 30 min prior to the photolysis and sealed from the ambient air during irradiation. The typical background $O_2$ concentration in the $N_2$-purged suspension was less than 10 $\mu$M (measured by a dissolved oxygen meter) and maintained at this level throughout the photolysis.

Photoirradiation employed a 300-W Xe arc lamp (Oriel) as a light source. Light passed through a 10-cm IR water filter and a UV cutoff filter ($\lambda$ > 295 nm for UV irradiation or $\lambda$ > 420 nm for visible irradiation), and then the filtered light was focused onto a 30-mL Pyrex reactor with a quartz window. When the wavelength-dependent photocatalytic reactivities were investigated, a series of long-pass cutoff filters were used. The reactor was filled with minimized headspace and stirred magnetically. Sample aliquots were withdrawn from the reactor intermittently during the illumination and filtered through a 0.45-$\mu$m polytetrafluoroethylene (PTFE) syringe filter (Millipore). Multiple photolysis experiments were performed under the identical reaction conditions to confirm the reproducibility.

The degradation of 4-CP was monitored using high-performance liquid chromatography (HPLC, Agilent 1100 series) equipped with a diode array detector and a ZORBAX 300SB C18 column (4.6 mm × 150 mm). The eluent was a binary mixture of water containing 0.1% phosphoric acid and acetonitrile (80:20 by volume). Identification and quantification of DCA and chloride ions were performed by using an ion chromatograph (IC, Dionex DX-120) that was equipped with a Dionex IonPac AS 14 (4 mm × 250 mm) column and a conductivity detector. The eluent solution was 3.5 mM $Na_2CO_3$/1 mM $NaHCO_3$.

## Results and Discussion

**Characterization of Pt-Ion-Doped $TiO_2$.** The redox energy states of many transition metal ions fall in the band gap region of $TiO_2$, and the substitution of Pt ions into the $TiO_2$ lattice should create defect sites in the band gap. The electronic transition between the defect energy states and the band edge (CB or VB) should be responsible for the visible light absorption of $Pt_{ion}-TiO_2$ (yellow-brown). Figure 1a compares the diffuse reflectance UV−vis spectra of $Pt_{ion}-TiO_2$ with varying Pt ion content, which clearly shows that the visible absorption ($\lambda$ > 400 nm) increases with the Pt content. Figure 1b is an alternative representation ($[KM\cdot E]^{1/2}$ vs $E$) of the absorption spectra (KM vs $\lambda$; Figure 1a) on the basis of the assumption that $Pt_{ion}-TiO_2$ is a semiconductor with an indirect band gap like $TiO_2$.[2] The extrapolation of the linear portion of the modified spectra to zero absorption determines the band gap energies of $Pt_{ion}-TiO_2$, which are estimated as 2.7−2.8 and 3.0 eV for 2.0−0.2% Pt-ion-doped and undoped $TiO_2$, respectively. The visible light

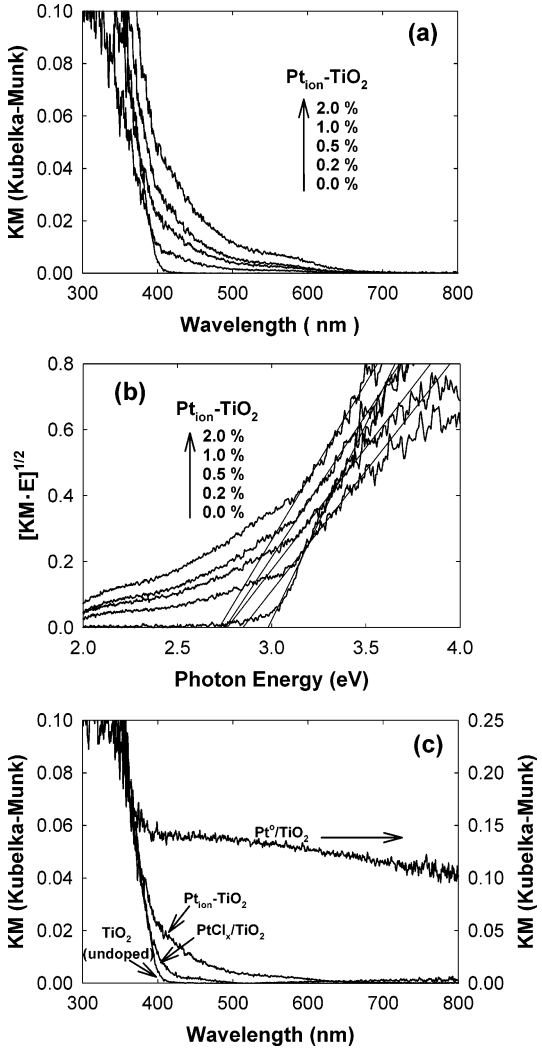


**Figure 1.** (a) Diffuse reflectance UV/vis spectra of $Pt_{ion}-TiO_2$ as a function of the Pt content. (b) Plot of the modified Kubelka−Munk (KM) function versus photon energy ($E$) for the reflectance spectra of $Pt_{ion}-TiO_2$ samples. (c) Comparison of the diffuse reflectance spectra of $Pt_{ion}-TiO_2$ with $Pt^0/TiO_2$ and $PtCl_x/TiO_2$.

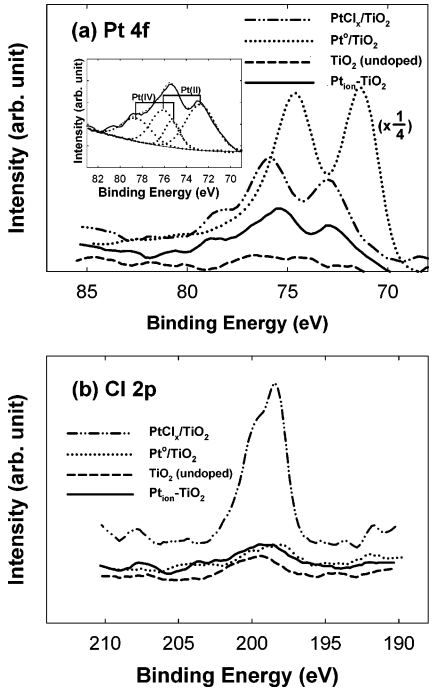


**Figure 2.** XPS spectra of various Pt-modified $TiO_2$ samples in the (a) Pt 4f and (b) Cl 2p band region. The Pt content in all samples was the same at 0.5 atom %.

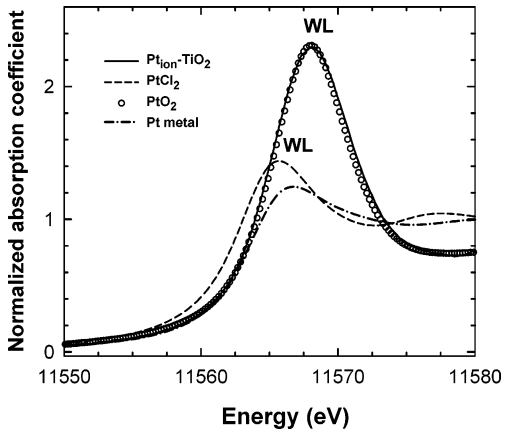


**Figure 3.** Pt $L_{III}$ edge XANES spectrum for the $Pt_{ion}-TiO_2$ compound (solid lines), in comparison with those for the references $PtO_2$ (circles), $PtCl_2$ (dashed lines), and Pt metal (dot−dashed lines).

absorption background below 2.7 eV (or above 460 nm) in $Pt_{ion}-TiO_2$ should be ascribed to the electronic transition between the Pt redox states and the band edge not to the band gap transition.

The diffuse reflectance spectrum of $Pt_{ion}-TiO_2$ is clearly distinguished from that of $Pt^0/TiO_2$ and $PtCl_x/TiO_2$ as shown in Figure 1c, although the total Pt content was similar among these Pt-modified $TiO_2$ samples. The reflectance spectrum of $Pt^0/TiO_2$ exhibits a significant background in the visible region, which is a characteristic optical property of Pt metal/$TiO_2$ composite.[36] The visible light absorption of $PtCl_x/TiO_2$ was much weaker than that of $Pt_{ion}-TiO_2$ at the same level of Pt content. The differences among these Pt-modified samples are also revealed from the XPS analysis. Figure 2 compares the XPS spectra of $Pt_{ion}-TiO_2$, $Pt^0/TiO_2$, and $PtCl_x/TiO_2$ for the Pt 4f and Cl 2p bands. The oxidation states of Pt species are clearly different among them. The Pt(0) state is dominant with $Pt^0/TiO_2$ whereas Pt(II) and Pt(IV) prevail with $Pt_{ion}-TiO_2$ and $PtCl_x/TiO_2$. The inset in Figure 2a shows the deconvoluted Pt 4f band of $Pt_{ion}-TiO_2$, which indicates the presence of Pt(II) and Pt(IV) states. The Pt(II)/Pt(IV) concentration ratio is 2.0. As for $PtCl_x/TiO_2$, the ratio of Pt(II)/Pt(IV) is 1.0, which is consistent with the previous report that the platinum-chloride-modified $TiO_2$ has Pt(IV) as a main species.[37] The surface chlorides are present only with $PtCl_x/TiO_2$ and absent with other samples (Figure 2b). However, it should be noted that, due to the sensitivity of XPS to the surface state, the present XPS results mainly reflect the chemical environment of Pt ions on the sample surface, not in the bulk state.[38] In this regard, we have examined the electronic and local crystal structures of doped Pt ions in $Pt_{ion}-TiO_2$ with an XAS technique that can provide information on the bulk state. The Pt $L_{III}$ edge XANES spectrum of $Pt_{ion}-TiO_2$ is presented in Figure 3, in comparison with the reference spectra of $PtO_2$, $PtCl_2$, and Pt metal. All of the present compounds show an intense white line (WL) corresponding to a $2p \rightarrow 5d$ transition, whose intensity is proportional to the density of the unoccupied final 5d states.[39] As shown in Figure 3, there is a systematic correlation between the WL intensity and the oxidation state of Pt in the reference compounds under investigation, since the hole density in the 5d orbital becomes larger with the increasing oxidation state of platinum: Pt(IV) = $5d^6$, Pt(II) = $5d^8$, Pt(0) = $5d^9$. In this regard, the nearly identical intensity of the WL

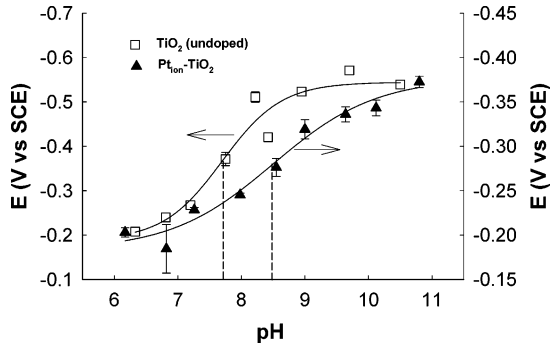


**Figure 4.** Methyl-viologen-mediated photovoltage developed in the UV-illuminated suspension of photocatalyst as a function of pH. The dashed lines indicate the position of inflection points.

for $Pt_{ion}-TiO_2$ and $PtO_2$ provides strong evidence that Pt(IV) is prevalent in $Pt_{ion}-TiO_2$. In addition, the overall spectral feature of $Pt_{ion}-TiO_2$ is nearly identical to that of the reference $PtO_2$, which suggests that Pt ions are incorporated into the oxide lattice. In contrast to the XPS results mentioned above, the XAS analysis rules out the presence of Pt(II) ions within the bulk lattice of $Pt_{ion}-TiO_2$. Such an inconsistency between both analyses is due to the sensitivity of XPS to the surface species and that of XAS to the bulk ones.[38] The XPS peaks at low binding energies corresponding to divalent oxidation states can be regarded as a proof on the partial formation of Pt(II) ions on the surface. It is highly feasible that coordinatively unsaturated sites on the surface, for instance, a pseudo-square-planar site, would stabilize the lower oxidation state of Pt(II). This speculation could be further supported from a comparison of the ion sizes of related cations ($Pt^{2+}(6) = 0.94$ Å, $Pt^{4+}(6) = 0.765$ Å, and $Ti^{4+}(6) = 0.745$ Å, where the number in parentheses represents the coordination number);[40] a significant size difference between Pt(II) and Ti(IV) ions would prevent effectively the incorporation of Pt(II) ions into the titanium site of the $TiO_2$ lattice.

The flat band potentials ($E_{fb}$) of $Pt_{ion}-TiO_2$ and undoped $TiO_2$ were determined by the $MV^{2+}$-mediated photovoltage measurement in the suspension state.[34,35] Figure 4 shows the variation of the photovoltage developed in $Pt_{ion}-TiO_2$ and $TiO_2$ suspension as a function of pH. The inflection point corresponds to the pH ($pH_0$) where the Fermi level of $TiO_2$ particles is equal to the standard reduction potential of methyl viologen ($E°(MV^{2+}/MV^{+}) = -0.445$ $V_{NHE}$). From this, $E_{fb}$ at a specific pH can be obtained from the following equation

$$E_{fb}(pH) = -0.445 + 0.059 \quad (pH_0 - pH) \quad (V \text{ vs NHE}) \tag{1}$$

The $E_{fb}$ values at pH 3 (typical reaction pH employed in this study) were determined to be $-0.12$ and $-0.17$ $V_{NHE}$ for $Pt_{ion}-TiO_2$ and $TiO_2$, respectively. The positive shift by 50 mV in $E_{fb}$ indicates that the CB edge position in $Pt_{ion}-TiO_2$ is slightly lowered. Such a shift is comparable in its magnitude to that observed with carbon-doped $TiO_2$ and nitrogen-doped $TiO_2$.[22,24]

The HRTEM images and EDX spectra of $Pt_{ion}-TiO_2$ and $Pt^0/TiO_2$ are compared in Figure 5. The Pt phase is clearly seen as

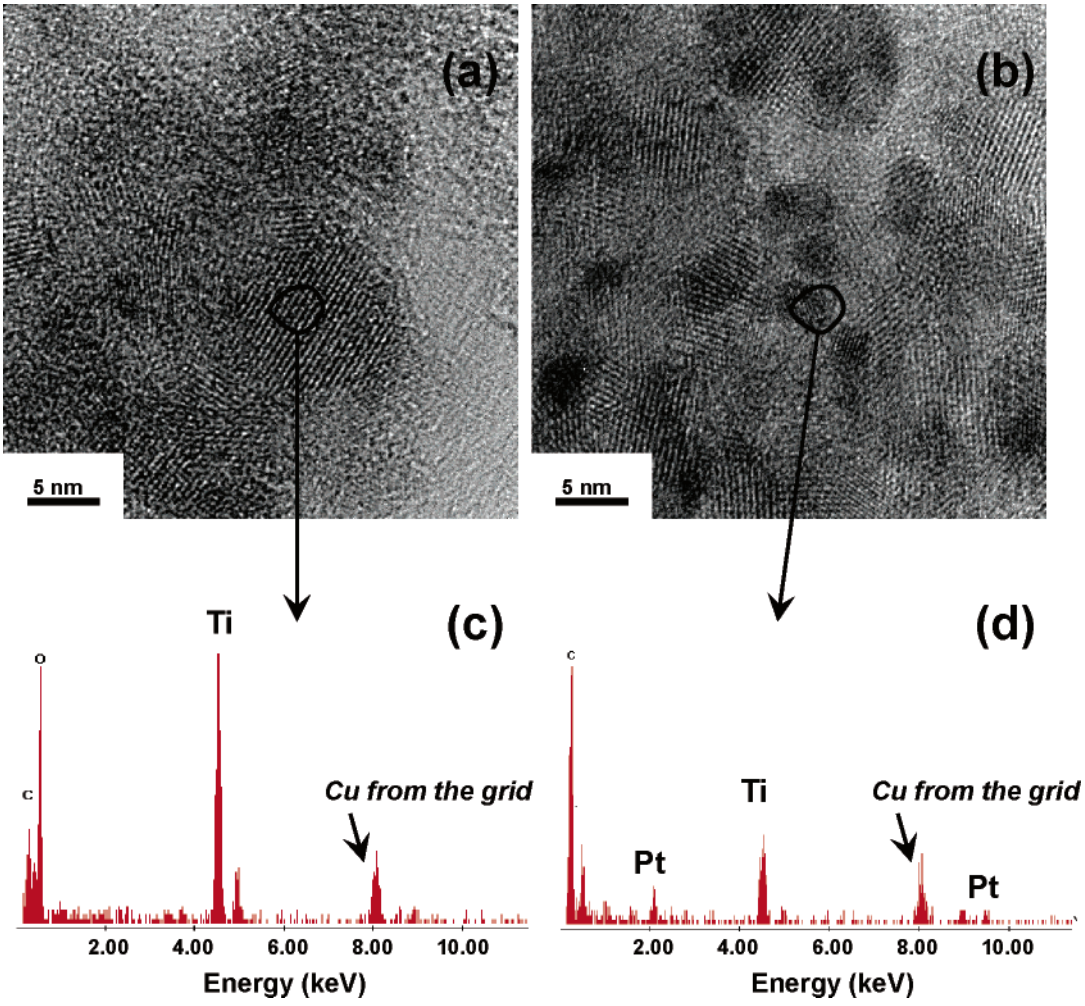


**Figure 5.** High-resolution TEM images (a and b) and energy-dispersive X-ray spectra (c and d) of $Pt_{ion}-TiO_2$ (a and c) and $Pt^0/TiO_2$ (b and d).

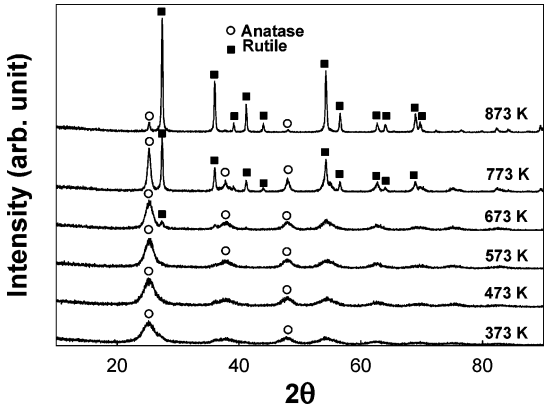


**Figure 6.** X-ray diffractograms of $Pt_{ion}-TiO_2$ (Pt content 0.5 atom %) samples calcined at different temperatures.

a dark spot with $Pt^0/TiO_2$ (Figure 5b) but not with $Pt_{ion}-TiO_2$ (Figure 5a). The EDX analysis exhibits a clear Pt signal with $Pt^0/TiO_2$ whereas it was hardly observed with $Pt_{ion}-TiO_2$ even though both samples contained the same content of Pt. This indicates that the Pt ions are well dispersed in the $TiO_2$ lattice and not concentrated in the surface region. In this context, the intensity of the Ti signal is weaker with $Pt^0/TiO_2$ because the surface of $TiO_2$ is covered with Pt metal.

The XRD analysis of $Pt_{ion}-TiO_2$ samples calcined at various temperatures shows that the anatase phase was dominant up to 673 K, above which the phase transformation to rutile started and nearly finished at 873 K (Figure 6). No diffraction peaks other than those of anatase and rutile were found, which indicates that the substitution of Pt ions into the $TiO_2$ lattice did not induce the formation of separate impurity phases (e.g., platinum oxide, platinum metal). The particle sizes that were estimated from the X-ray peak width (using the Scherrer equation) were 7−8 nm up to 673 K and increased to 18.3 and 26.8 nm (for anatase) and 31.1 and 33.7 nm (for rutile) at 773 and 873 K, respectively. The visible light activity of $Pt_{ion}-TiO_2$ was sensitively influenced by the calcination temperature. As for the degradation of DCA, the visible light reactivity of $Pt_{ion}-TiO_2$ rapidly increased with the calcination temperature and was optimized at 673 K (Figure 7a). However, the calcination temperature-dependent activity for 4-CP degradation was markedly different: The activity was relatively constant in the 373−673 K range, which implies that the visible-light-induced degradation mechanisms are different between DCA and 4-CP. The most plausible explanation is that the degradation of 4-CP can be mediated not only by VB hole oxidation but also by a surface-complex-mediated path that does not require the band gap excitation.[41] It seems that the charge recombination rate is minimized with $Pt_{ion}-TiO_2$ calcined at 673 K, and hence the activity for DCA degradation (mediated by VB holes) was maximal at this condition. However, the surface-complex-mediated degradation of 4-CP on $Pt_{ion}-TiO_2$ should not be influenced by the charge recombination process, and consequently the activity for 4-CP degradation is not reduced at lower calcination temperature. However, the visible light absorption by the $Pt_{ion}-TiO_2$ samples was generally higher with those calcined at a higher temperature as shown in Figure 7b. However, the samples calcined at 773 K and higher were almost completely inactive despite the higher visible absorption probably because the surface area was drastically reduced at these calcination temperatures (Figure 7a). The optimum concentration of Pt ion dopant was found to be 0.5 atom % for DCA degradation whereas the activity for 4-CP degradation depended little on the Pt content in the 0.5−2.0 atom % range (Figure 7c). It has been frequently reported that the optimum concentrations of metal ion dopants in $TiO_2$ photocatalysts are in this range.[10] In the following reactivity measurements, the $Pt_{ion}-TiO_2$ sample with 0.5 atom % Pt and calcined at 673 K was used as a standard catalyst.

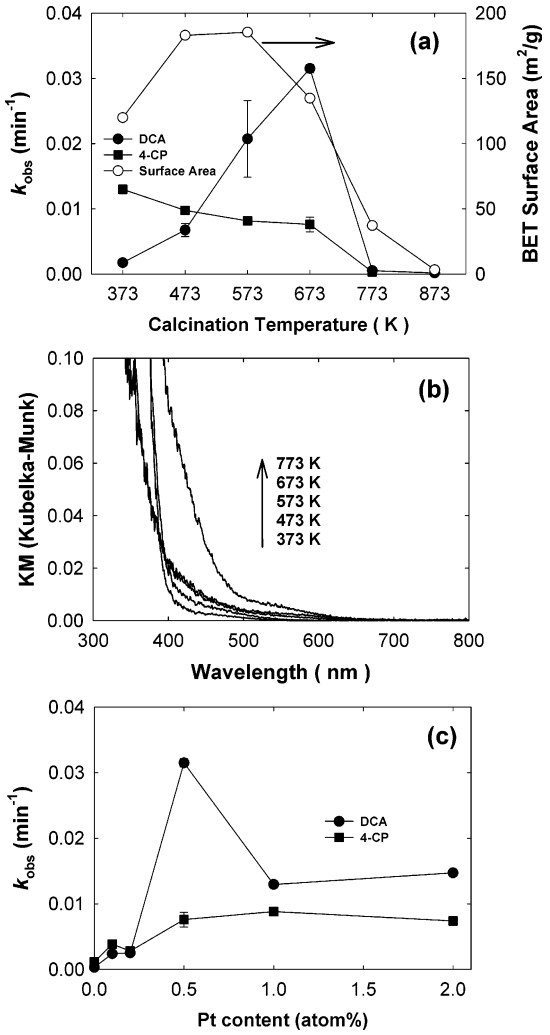


**Figure 7.** (a) Visible-light-induced PCD rates of DCA and 4-CP as a function of calcination temperature of $Pt_{ion}-TiO_2$ (0.5 atom % Pt). The change of BET surface area of $Pt_{ion}-TiO_2$ as a function of calcination temperature is also compared in part a. (b) Diffuse reflectance spectra of $Pt_{ion}-TiO_2$ (0.5 atom % Pt) calcined at different temperatures. (c) Visible PCD rates as a function of the Pt content in $Pt_{ion}-TiO_2$ (calcined at 673 K).

**Visible Light Activities of $Pt_{ion}-TiO_2$.** The photocatalytic activities of various Pt-modified $TiO_2$ samples were tested with respect to the degradation of organic compounds. Figure 8 compares the time-dependent chloride production from the degradation of DCA under UV ($\lambda$ > 320 nm) or visible ($\lambda$ > 420 nm) irradiation among $Pt_{ion}-TiO_2$, $Pt^0/TiO_2$, $PtCl_x/TiO_2$, and undoped $TiO_2$. All Pt-modified $TiO_2$ samples were more active than undoped $TiO_2$ and comparable to P25 (the most popular commercial $TiO_2$ photocatalyst) under UV irradiation (Figure 8a). Under visible irradiation (Figure 8b), only $Pt_{ion}-TiO_2$ and $PtCl_x/TiO_2$ showed the activity: The former was more active than the latter. The visible light activity of $PtCl_x/TiO_2$ has been previously ascribed to the sensitizing action of platinum chloride complexes.[37] The chloride generation with $PtCl_x/TiO_2$ was quantitatively balanced with the removal of DCA, which indicates that most chlorides came from DCA degradation, not from the degradation of platinum chlorides on $TiO_2$.

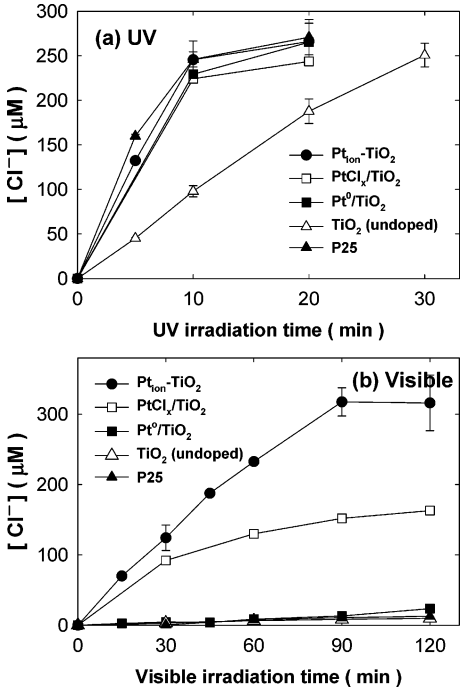


**Figure 8.** Chloride production from the degradation of DCA ($C_0$ = 130−150 $\mu$M) under (a) UV and (b) visible irradiation with various photocatalysts. The Pt content in all Pt-modified samples was the same at 0.5 atom %. All suspensions (pH 3) were equilibrated with air.

The impurity doping in the $TiO_2$ lattice either inhibits or enhances the photocatalytic activity depending on the role of dopants (recombination center vs charge trap). Choi et al.[10] showed that doping $TiO_2$ nanoparticles with $Fe^{3+}$, $Mo^{5+}$, $Ru^{3+}$, $Os^{3+}$, $Re^{3+}$, $V^{4+}$, and $Rh^{3+}$ significantly increases the photoreactivity while $Co^{3+}$ and $Al^{3+}$ doping decreases it. Since the UV photocatalytic activity of $Pt_{ion}-TiO_2$ is markedly enhanced from that of undoped $TiO_2$, the doped Pt ions ($Pt^{4+}$ as a major component in the bulk with some $Pt^{2+}$ on the surface according to the XAS and XPS results) should serve mainly as an inhibitor of recombination by trapping electrons or holes (reactions 3 and 4), not as a recombination center (reactions 5 and 6). The trapped charges directly transfer to the surface or hop from a defect site to another successively to reach the surface to initiate photocatalysis.

$$TiO_2 + h\nu \rightarrow e_{cb}^- + h_{vb}^+ \text{ (excitation)} \quad (2)$$

$$Pt^{4+} + e_{cb}^- \rightarrow Pt^{3+} \text{ (electron trapping)} \quad (3)$$

$$Pt^{2+} + h_{vb}^+ \rightarrow Pt^{3+} \text{ (hole trapping)} \quad (4)$$

$$Pt^{4+} + e_{cb}^- + h_{vb}^+ \rightarrow Pt^{4+} \text{ (trap-mediated recombination)} \quad (5)$$

$$Pt^{2+} + h_{vb}^+ + e_{cb}^- \rightarrow Pt^{2+} \text{ (trap-mediated recombination)} \quad (6)$$

However, the visible activity of $Pt_{ion}-TiO_2$ should be ascribed to the role of doped Pt ions as a charge generating center (reactions 7 and 8), which produces free and trapped charges ($Pt^{3+}$). Some trapped charges may recombine to regenerate the initial redox states (reaction 9). The visible-light-induced VB holes or trapped holes may subsequently react with DCA (reactions 10 and 11).

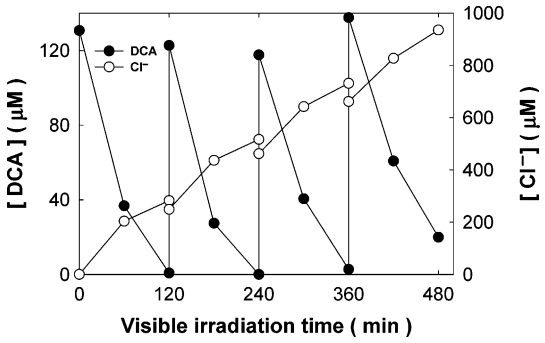


**Figure 9.** Repeated cycles of DCA degradation and the concurrent chloride production in visible-light-illuminated $Pt_{ion}-TiO_2$ suspension. The small drops in the chloride concentration at the beginning of each cycle were due to dilution when an aliquot of DCA stock solution was added.

$$Pt^{4+} + h\nu \rightarrow Pt^{3+} \text{ (or trapped electron)} + h_{vb}^+ \quad (7)$$

$$Pt^{2+} + h\nu \rightarrow Pt^{3+} \text{ (or trapped hole)} + e_{cb}^- \quad (8)$$

$$Pt^{3+} + Pt^{3+} \rightarrow Pt^{2+} + Pt^{4+} \text{ (recombination via tunneling)} \quad (9)$$

$$CHCl_2CO_2^- + h_{vb}^+ \rightarrow {}^\bullet CHCl_2 + CO_2 \quad (10)$$

$$CHCl_2CO_2^- + Pt^{3+} \rightarrow {}^\bullet CHCl_2 + CO_2 + Pt^{2+} \quad (11)$$

In addition, to test the stability of $Pt_{ion}-TiO_2$, the DCA degradation under visible irradiation was repeated with using the same catalyst as shown in Figure 9. The visible light reactivity showed little sign of deactivation up to four repeated cycles, which implies that the initial oxidation states of Pt ions are maintained during the photocatalysis.

Figure 10 shows that 4-CP and TCA could be also degraded under visible light with $Pt_{ion}-TiO_2$. The degradation of 4-CP was accompanied by the stoichiometric production of chloride, and the total organic carbon (TOC) content was reduced by 49% in 2 h of irradiation. The slow degradation of 4-CP with undoped $TiO_2$ under visible light is not due to the presence of trace UV light but due to the surface-complex-mediated path as mentioned earlier.[41] To test whether OH radicals are generated on the visible-light-illuminated $Pt_{ion}-TiO_2$, an excess of *tert*-butyl alcohol (TBA) was added as an OH radical scavenger (Figure 10a). Under UV irradiation, the addition of TBA significantly reduced the degradation rate of 4-CP since OH radicals were involved as an oxidant.[41] In this case, however, the presence of TBA little affected the degradation rate of 4-CP, which implies that the visible PCD process taking place on $Pt_{ion}-TiO_2$ seems to be mediated not by OH radicals but by a direct charge transfer in a similar way as in reactions 10 and 11. The degradation of 4-CP did not occur at all in the $N_2$-saturated condition, which rules out the possibility of a reductive dechlorination mechanism (i.e., electron-transfer-mediated) in 4-CP degradation under visible light. 4-CP should be degraded through a hole-mediated path.

To test the photoreductive activity of $Pt_{ion}-TiO_2$, the degradation of TCA under visible light was measured (Figure 10b). From previous studies,[29,42] it is known that the photocatalytic degradation of TCA should be initiated by a reductive electron transfer (reaction 12). Both oxic and anoxic pathways

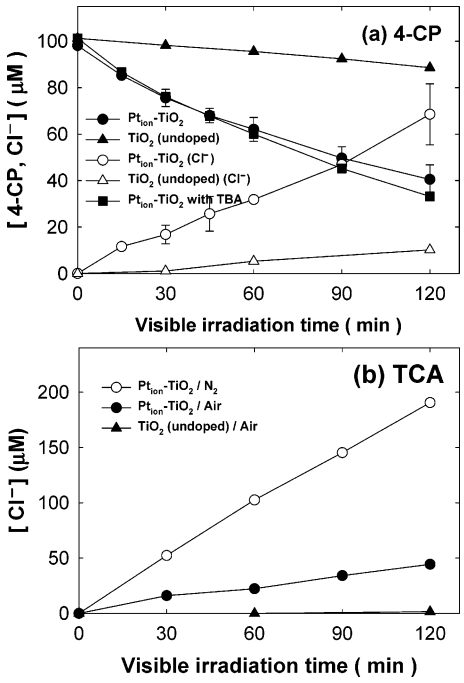


**Figure 10.** Visible PCD of (a) 4-CP and (b) TCA with $Pt_{ion}-TiO_2$ (0.5 atom % Pt). $[4\text{-CP}]_0 = [TCA]_0 = 100\ \mu M$, $[TBA]_0 = 1$ M (when indicated).

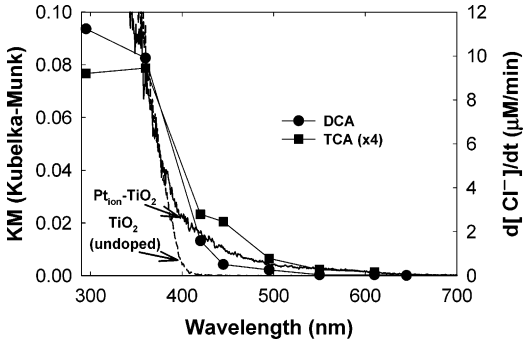


**Figure 11.** Wavelength-dependent PCDs (chloride production) of DCA (under air equilibration) and TCA (under $N_2$ saturation) compared with the diffuse reflectance spectra of $Pt_{ion}-TiO_2$ (0.5 atom %).

for the further degradation of the dichloroacetate radical are known (reactions 14 and 15).

$$CCl_3CO_2^- + e_{cb}^- \rightarrow {}^{\bullet}CCl_2CO_2^- + Cl^- \quad (12)$$

$$O_2 + e_{cb}^- \rightarrow O_2^- \quad (13)$$

$${}^{\bullet}CCl_2CO_2^- + O_2 \rightarrow {}^{\bullet}OOCCl_2CO_2^- \rightarrow \rightarrow 2Cl^- \quad (14)$$

$${}^{\bullet}CCl_2CO_2^- + h_{vb}^+ \rightarrow CCl_2 + CO_2 \quad (15)$$

The degradation of TCA on UV-illuminated pure $TiO_2$ proceeds more rapidly in the presence of $O_2$ than in the absence of $O_2$ because the oxic path (reaction 14) prevails.[29] However, the visible-light-induced degradation of TCA with $Pt_{ion}-TiO_2$ is much favored in the anoxic condition, which implies that reaction 15 is favored. The fact that TCA can be successfully degraded with $Pt_{ion}-TiO_2$ in the absence of $O_2$ implies that both electrons (reaction 12) and holes (reaction 15) are involved in the overall reaction.

Figure 11 compares the photocatalytic activities of $Pt_{ion}-TiO_2$ for the degradation of DCA and TCA as a function of the irradiation wavelength. The diffuse reflectance spectra of $Pt_{ion}-TiO_2$ and undoped $TiO_2$ are compared along with the wavelength-dependent PCD rate. The visible light absorption profile is very similar to the wavelength-dependent profiles of PCD activity, which confirms that both oxidation (DCA degradation) and reduction (TCA degradation) are initiated by visible light activation of $Pt_{ion}-TiO_2$.

Finally, it should be mentioned that the visible PCD activity of $Pt_{ion}-TiO_2$ prepared in this study is rather limited compared with the UV PCD activity of $TiO_2$. For example, the tetramethylammonium (TMA) and trichloroethylene could not be degraded at all with $Pt_{ion}-TiO_2$ under visible light whereas they could be successfully degraded with UV-illuminated $TiO_2$.[43,44] Incidentally, TMA is suggested as a probe substrate to test whether a photocatalyst can generate OH radicals or not under UV or visible irradiation. TMA is a very recalcitrant molecule and hardly adsorbs on the metal oxide surface. Therefore, its degradation should be initiated only by an OH radical, not by a direct hole transfer. Nitrogen-doped $TiO_2$ that is widely used as one of the most successful visible active photocatalysts also lacks of oxidative power and could not oxidize formates that are readily degraded on UV-illuminated $TiO_2$.[45]

## Conclusions

Photocatalytic materials that have visible light activity are of paramount importance as essential elements of solar photoenergy conversion. Diverse approaches are being made in search of visible light active photocatalysts. In this study we prepared $Pt_{ion}-TiO_2$ as a new kind of visible light active photocatalyst and demonstrated its visible activity in various ways. Although Pt-metal-loaded $TiO_2$ has been frequently investigated as a modified $TiO_2$ photocatalyst, Pt-ion-doped $TiO_2$ that exhibits visible light activity has not been studied yet in detail. Visible light absorption by $Pt_{ion}-TiO_2$ is ascribed to the electronic transition between the band edge (CB or VB) and the defect redox states of Pt ions substituted into the $TiO_2$ lattice. The main oxidation states of Pt ions in the bulk lattice of $TiO_2$ were Pt(IV) whereas there are some Pt(II) species on the surface. The visible light activity of $Pt_{ion}-TiO_2$ was clearly distinguished from that of $Pt^0/TiO_2$ and $PtCl_x/TiO_2$. $Pt_{ion}-TiO_2$ exhibited photocatalytic activities for both oxidative and reductive degradation of selected chlorinated organic compounds. However, the number of substrates that can be degraded by $Pt_{ion}-TiO_2$ under visible light is limited compared with UV-induced photocatalysis. It should be realized that we get less redox power under visible excitation at the expense of utilizing low energy photons, which limits the range of redox reactions that can be driven photocatalytically. This should be true for visible light photocatalysis in general. Overall, $Pt_{ion}-TiO_2$ prepared in this study seems to be promising as a new visible light active photocatalyst like nitrogen-doped and carbon-doped $TiO_2$.

**Acknowledgment.** This work was supported by the Korea Institute of Science and Technology, the Daegu Gyeongbuk Institute of Science and Technology, and the SRC/ERC program of the MOST/KOSEF (Grant No. R11-2000-070-06004-0).

## References and Notes

(1) Hoffmann, M. R.; Martin, S. T.; Choi, W.; Bahnemann, D. W. *Chem. Rev.* **1995**, *95*, 69.

(2) *Photocatalysis—Fundamentals and Applications*; Wiley-Interscience: New York, 1989.

(3) Duonghong, D.; Borgarello, E.; Gratzel, M. *J. Am. Chem. Soc.* **1981**, *103*, 4685.

(4) (a) Cho, Y.; Choi, W.; Lee, C.-H.; Hyeon, T.; Lee, H.-I. *Environ. Sci. Technol.* **2001**, *35*, 966. (b) Bae, E.; Choi, W. *Environ. Sci. Technol.* **2003**, *37*, 147. (c) Bae, E.; Choi, W.; Park, J.; Shin, H. S.; Kim, S. B.; Lee, J. S. *J. Phys. Chem. B* **2004**, *108*, 14093.

(5) Spanhel, L.; Weller, H.; Henglein, A. *J. Am. Chem. Soc.* **1987**, *109*, 6632.

(6) Gopidas, K. R.; Bohorquez, M.; Kamat, P. V. *J. Phys. Chem.* **1990**, *94*, 6435.

(7) Nasr, C.; Kamat, P. V.; Hotchandani, S. *J. Phys. Chem. B* **1998**, *102*, 10047.

(8) Borgarello, E.; Kiwi, J.; Grätzel, M.; Pelizzetti, E.; Visca, M. *J. Am. Chem. Soc.* **1982**, *104*, 2996.

(9) Moser, J.; Grätzel, M.; Gallay, R. *Helv. Chim. Acta* **1987**, *70*, 1596.

(10) Choi, W.; Termin, A.; Hoffmann, M. R. *J. Phys. Chem.* **1994**, *98*, 13669.

(11) Wilke, K.; Breuer, H. D. *J. Photochem. Photobiol., A* **1999**, *121*, 49.

(12) Ikeda, S.; Sugiyama, N.; Pal, B.; Marci, G.; Palmisano, L.; Noguchi, H.; Uosaki, K.; Ohtani, B. *Phys. Chem. Chem. Phys.* **2001**, *3*, 267.

(13) Paola, A. D.; Marci, G.; Palmisano, L.; Schiavello, M.; Uosaki, K.; Ikeda, S.; Ohtani, B. *J. Phys. Chem. B* **2002**, *106*, 637.

(14) Ohno, T.; Tanigawa, F.; Fujihara, K.; Izumi, S.; Masumura, M. *J. Photochem. Photobiol., A* **1999**, *127*, 107.

(15) Zhao, G.; Kozuka, H.; Lin, H.; Yoko, T. *Thin Solid Films* **1999**, *339*, 123.

(16) Klosek, S.; Raftery, D. *J. Phys. Chem. B* **2001**, *105*, 2815.

(17) Li, X. Z.; Li, F. B. *Environ. Sci. Technol.* **2001**, *35*, 2381.

(18) Fuerte, A.; Hernandez-Alonso, M. D.; Maira, A. J.; Martinez-Arias, A.; Fernandez-Garcia, M.; Conesa, J. C.; Soria, J. *Chem. Commun.* **2001**, 2718.

(19) Xie, Y.; Yuan, C. *Appl. Surf. Sci.* **2004**, *221*, 17.

(20) Martin, S. T.; Morrison, C. L.; Hoffmann, M. R. *J. Phys. Chem.* **1994**, *98*, 13695.

(21) Asahi, R.; Morikawa, T.; Ohwaki, T.; Aoki, K.; Taga, Y. *Science* **2001**, *293*, 269.

(22) Sakthivel, S.; Kisch, H. *Angew. Chem., Int. Ed.* **2003**, *42*, 4908.

(23) Umebayashi, T.; Yamaki, T.; Tanaka, S.; Asai, K. *Chem. Lett.* **2003**, *32*, 330.

(24) Sakthivel, S.; Kisch, H. *ChemPhysChem* **2003**, *4*, 487.

(25) Burda, C.; Lou, Y.; Chen, X.; Samia, A. C. S.; Stout, J.; Gole, J. L. *Nano Lett.* **2003**, *3*, 1049.

(26) Gole, J. L.; Stout, J. D.; Burda, C.; Lou, Y.; Chen, X. *J. Phys. Chem. B* **2004**, *108*, 1230.

(27) Zhao, W.; Ma, W.; Chen, C.; Zhao, J.; Shuai, Z. *J. Am. Chem. Soc.* **2004**, *126*, 4782.

(28) Kraeutler, B.; Bard, A. J. *J. Am. Chem. Soc.* **1978**, *100*, 4317.

(29) Kim, S.; Choi, W. *J. Phys. Chem. B* **2002**, *106*, 13311.

(30) (a) Lee, J.; Park, H.; Choi, W. *Environ. Sci. Technol.* **2002**, *36*, 5462. (b) Lee, J.; Choi, W. *Environ. Sci. Technol.* **2004**, *38*, 4026. (c) Lee, J.; Choi, W. *J. Phys. Chem. B* **2005**, *109*, 7399.

(31) Lettmann, C.; Hinrichs, H.; Maier, W. F. *Angew. Chem., Int. Ed.* **2001**, *40*, 3160.

(32) (a) Burgeth, G.; Kisch, H. *Coord. Chem. Rev.* **2002**, *230*, 41. (b) Macyk, W.; Kisch, H. *Chem.—Eur. J.* **2001**, *7*, 1862. (c) Zang, L.; Macyk, W.; Lange, C.; Maier, W. F.; Antonius, C.; Meissner, D.; Kisch, H. *Chem.—Eur. J.* **2000**, *6*, 379. (d) Kisch, H.; Zang, L.; Lange, C.; Maier, W. F.; Antonius, C.; Meissner, D. *Angew. Chem., Int. Ed. Engl.* **1998**, *37*, 3034.

(33) Choy, J. H.; Hwang, S. J.; Park, M. G. *J. Am. Chem. Soc.* **1997**, *119*, 1624.

(34) Roy, A. M.; De, G. C.; Sasmal, N.; Bhattacharyya, S. S. *Int. J. Hydrogen Energy* **1995**, *20*, 627.

(35) Ward, M. D.; White, J. R.; Bard, A. J. *J. Am. Chem. Soc.* **1983**, *105*, 27.

(36) Driessen, M. D.; Grasian, V. H. *J. Phys. Chem. B* **1998**, *102*, 1418.

(37) Zang, L.; Lange, C.; Abraham, I.; Storck, S.; Maier, W. F.; Kisch, H. *J. Phys. Chem. B* **1998**, *102*, 10765.

(38) Treuil, N.; Labrugère, C.; Menetrier, M.; Portier, J.; Campet, G.; Deshayes, A.; Frison, J. C.; Hwang, S. J.; Song, S. W.; Choy, J. H. *J. Phys. Chem. B* **1999**, *103*, 2100.

(39) Sinfelt, J. H.; Meitzner, G. D. *Acc. Chem. Res.* **1993**, *26*, 1.

(40) Shannon, R. D. *Acta Crystallogr., Sect. A* **1976**, *32*, 751.

(41) Kim, S.; Choi, W. *J. Phys. Chem. B* **2005**, *109*, 5143.

(42) Choi, W.; Hoffmann, M. R. *Environ. Sci. Technol.* **1997**, *31*, 89.

(43) Kim, S.; Choi, W. *Environ. Sci. Technol.* **2002**, *36*, 2019.

(44) Kim, S.; Park, H.; Choi, W. *J. Phys. Chem. B* **2004**, *108*, 6402.

(45) Mrowetz, M.; Balcerski, W.; Colussi, A. J.; Hoffmann, M. R. *J. Phys. Chem. B* **2004**, *108*, 17269.